

LETTER • OPEN ACCESS

Mechanisms driving ESM-based marine ecosystem predictive skill on the east African coast

To cite this article: Woojin Jeon *et al* 2022 *Environ. Res. Lett.* **17** 084004

View the [article online](#) for updates and enhancements.

You may also like

- [Wintertime marine extreme temperature events modulate phytoplankton blooms in the North Pacific through subtropical mode water](#)
Yong-Jin Tak, Hajoong Song and Jong-Yeon Park
- [A mid-troposphere perspective on the East African climate paradox](#)
Thomas Mölg and Carolyne Pickler
- [Optimization of chlorophyll extraction solvent of bulung sangu \(*Gracilaria* sp.\) seaweed](#)
M M V Sasadara, N M D M W Nayaka, P E S K Yuda et al.

ENVIRONMENTAL RESEARCH
LETTERS

LETTER

Mechanisms driving ESM-based marine ecosystem predictive skill on the east African coast

OPEN ACCESS

RECEIVED

23 March 2022

REVISED


16 June 2022

ACCEPTED FOR PUBLICATION

30 June 2022

PUBLISHED

15 July 2022

Woojin Jeon^{1,2}, Jong-Yeon Park^{1,2,*} , Charles A Stock³, John P Dunne³, Xiaosong Yang³ and Anthony Rosati³¹ Department of Earth and Environmental Sciences, Jeonbuk National University, Jeonju, Jeollabuk-do, Republic of Korea² Department of Environment and Energy, Jeonbuk National University, Jeonju, Jeollabuk-do, Republic of Korea³ National Oceanic and Atmospheric Administration/Geophysical Fluid Dynamics Laboratory, Princeton, NJ, United States of America

* Author to whom any correspondence should be addressed.

E-mail: jongyeon.park@jbnu.ac.kr**Keywords:** marine biogeochemistry, Earth system model, chlorophyll predictionSupplementary material for this article is available [online](#)

Original content from this work may be used under the terms of the [Creative Commons Attribution 4.0 licence](#).

Any further distribution of this work must maintain attribution to the author(s) and the title of the work, journal citation and DOI.

**Abstract**

The extension of seasonal to interannual prediction of the physical climate system to include the marine ecosystem has a great potential to inform marine resource management strategies. Along the east coast of Africa, recent findings suggest that skillful Earth system model (ESM)-based chlorophyll predictions may enable anticipation of fisheries fluctuations. The mechanisms underlying skillful chlorophyll predictions, however, were not identified, eroding confidence in potential adaptive management steps. This study demonstrates that skillful chlorophyll predictions up to two years in advance arise from the successful simulation of westward-propagating off-equatorial Rossby waves in the Indian ocean. Upwelling associated with these waves supplies nutrients to the surface layer for the large coastal areas by generating north- and southward propagating waves at the east African coast. Further analysis shows that the off-equatorial Rossby wave is initially excited by wind stress forcing caused by El Niño/Southern Oscillation-Indian Ocean teleconnections.

1. Introduction

Marine ecosystems and the living resources they sustain are subject to pronounced climate-driven fluctuations that have long challenged sustainable marine resource management efforts (Finney *et al* 2010, Costello *et al* 2016, Tommasi *et al* 2017). These fluctuations are compounded by ocean warming, changing ocean productivity baselines, deoxygenation, and acidification, all of which potentially influence the distribution of marine habitat types, phenology, and functioning of marine ecosystems (Doney *et al* 2012, Cheung *et al* 2013, Glibert *et al* 2014, Dussin *et al* 2019, Kwiatkowski *et al* 2020). Although century-scale climate change assessments provide a scientific foundation for developing policy options, such long-term projections are not sufficient for the tactical management decisions on seasonal to multi-annual time-scales critical to long-term resilience. Thus, reliable tools to anticipate seasonal to multi-annual and longer-term changes in the interacting

physical, chemical, and biological processes are both required for holistic marine resource management.

Earth system models (ESMs), the most comprehensive climate models incorporating Earth's biogeochemical cycles, have the potential to predict phenomena emerging from diverse physical and biogeochemical processes, including marine ecosystem responses to climate variability (Watanabe *et al* 2011, Dufresne *et al* 2013, Dunne *et al* 2013, Lindsay *et al* 2014, Bonan and Doney 2018). Several recent studies have suggested that many critical drivers of marine ecosystems, including temperature, nutrients, oxygen, acidity and ocean productivity, may be predictable on seasonal to multiannual time horizons (Seferian *et al* 2014, Taboada *et al* 2019, Frolicher *et al* 2020). This promise has been verified through the recent integration of biogeochemical dynamics with physical climate assimilation and prediction systems (Park *et al* 2019). Extensive retrospective forecast experiments using an ESM revealed verifiable seasonal to multi-annual chlorophyll predictions

in many ocean areas, and promising relationships with fisheries fluctuations in several large coastal areas.

One of the strongest linkages between skillful chlorophyll predictions and reconstructed fisheries catch was found along the east coast of Africa (Park *et al* 2019). Skillful multi-year chlorophyll predictions within two large coastal areas spanning the east African coast were highly correlated with fluctuations of small pelagic fisheries up to three years in advance (after allowing for a one year lag for ocean productivity signals to manifest in the fishable stock). The mechanisms underlying skillful chlorophyll predictions, however, were not explored, eroding confidence in predictions in any adaptive management measures for the significant industrial and subsistence fisheries that they support. The present study addresses this by conducting a detailed analysis of prediction skill across 20 years of multi-annual reforecast experiments initialized every month. Given that the countries of these regions have started to develop a transboundary monitoring and assessment program to deal with marine environmental issues and regional management approaches (Ménard *et al* 2007, Hutchings *et al* 2009, Vousden 2016), the current study may provide a timely contribution to inform these efforts by characterizing the dynamical mechanisms underlying prediction skill of seasonal to multiyear chlorophyll variability.

2. Methods

2.1. Global marine biogeochemical prediction system

The global marine biogeochemical prediction system used in the present study is based on the ESM developed at the Geophysical Fluid Dynamics Laboratory (GFDL). The ESM is a fully coupled atmosphere-land-ocean-sea ice model integrated with the GFDL's marine ecosystem model, the Carbon, Ocean Biogeochemistry and Lower Trophics (COBALTs) (Stock *et al* 2014a, 2014b). COBALT, an intermediate complex biogeochemical model, simulates 33 tracers to resolve global-scale cycles of nitrogen, carbon, phosphorus, iron, oxygen, and silica with three explicit phytoplankton and three explicit zooplankton groups. The horizontal resolution of the ESM is 2.5° longitude \times 2° latitude for the atmosphere and land, and $1^\circ \times 1^\circ$ for the ocean, sea ice, and marine biogeochemistry. Each grid has 24 hybrid sigma/pressure vertical layers for the atmosphere and 50 vertical layers for the ocean.

The initial condition for the marine biogeochemical prediction system is produced from GFDL's data assimilation system, the ensemble-coupled data assimilation (ECDA) system (Chang *et al* 2013). The ECDA system assimilates both observed atmosphere and ocean states, including winds and temperature from the National Centers for Environmental

Prediction—Department of Energy Reanalysis 2 (Kanamitsu *et al* 2002), oceanic profiles from the World Ocean Database and Argo profiles, and the sea surface data from the National Oceanic and Atmospheric Administration's optimum interpolation SST v2 high resolution dataset (Reynolds *et al* 2007). The system employs an ensemble Kalman filter assimilation scheme and is integrated with the marine ecological model, COBALT, to reproduce historical ocean biogeochemical fields. The modeled oceanic and atmospheric fields are optimally constrained by observations to suppress the degradation of biogeochemical fields caused by momentum imbalances from equatorial data assimilation (Park *et al* 2018).

2.2. Retrospective forecast experiment and skill assessment

The retrospective forecasts are the same as the ones used in a recent study (Park *et al* 2019). The forecast experiments are initialized at the 1st day of every calendar month during 1991–2017 and run for two years with 12 ensemble members (supplementary figure 1). The initial conditions for this experiment are produced by data assimilative hindcasts from the ECDA-COBALT system as described above. A previous work has already shown that the global ocean biogeochemical variables produced by this assimilation system can capture well observed large-scale biogeochemical patterns and variability (Park *et al* 2018), providing the appropriate initial conditions for the biogeochemical prediction system. The anomalies of predicted biogeochemical variables are calculated relative to the lead-dependent climatology from the 27 year ensemble mean predictions for each initialization month, given that the full-field assimilation method used here generally leads to model drift toward its own preferred state once the prediction starts. All forecast data analyzed in this study are the ensemble mean of predicted variables.

Predicted chlorophyll anomalies are compared with satellite-retrieved chlorophyll concentrations. We used the satellite chlorophyll data from the two ocean color sensors, the Sea-viewing Wide Field-of-view Sensor and the Moderate Resolution Imaging Spectroradiometer (Esaías *et al* 1998, McClain *et al* 1998). The original chlorophyll data was binned to a grid of $9 \text{ km} \times 9 \text{ km}$, thus the data has been re-gridded onto a $1.0^\circ \times 1.0^\circ$ grid using a bi-linear interpolation method for computational efficiency. The median value of chlorophyll in each 1.0° grid is used in the interpolation process given the nearly log-normal distribution of ocean chlorophyll concentrations (Campbell 1995). Chlorophyll prediction skill is measured by the temporal anomaly correlation coefficient between the predicted and satellite-retrieved chlorophyll concentrations after taking logarithmic transformation. The significance test for the correlation skill uses the reduced number of effective degrees of freedom that is defined by the autocorrelations of a

time-varying field, providing a conservative significance threshold (Bretherton *et al* 1999).

Chlorophyll prediction skill is evaluated at the large marine ecosystems (LMEs) scale, by focusing on the two east African coast LMEs, the Agulhas Current and the Somali Current. The LMEs are ocean areas defined by ecological criteria including bathymetry, hydrography, productivity, and trophodynamics (Sherman 1991). These large coastal areas encompass regions from estuaries to the seaward boundaries of the continental shelf or of coastal current systems, in which the adaptive management strategy to environmental changes is important to facilitate sustainable marine resource utilization given their substantial socio-economic benefits (Sherman 2014, Tommasi *et al* 2017).

3. Result

3.1. Chlorophyll prediction skill in coastal LMEs

LME-scale marine biogeochemical prediction from the global marine biogeochemical prediction system is assessed by anomaly correlation coefficient between the predicted and satellite-retrieved chlorophyll during the period 1998–2018. Chlorophyll anomalies are averaged in each LME region after removing the climatological annual cycle. The correlation coefficient is calculated for each initialization month and lead time (see section 2).

The prediction system shows notable chlorophyll forecasting skill in the two African coastal LMEs, Agulhas current and Somali coastal current systems (figure 1; geographical locations of both LMEs are shown in supplementary figure 2). In the Agulhas Current system, significant chlorophyll prediction skill appears up to two years, with the alternating pattern of high- and low-prediction skills in diagonal bands corresponding to high predictability seasons (figure 1(a)). The skillful predictions are mostly possible in the austral winter and early spring regardless of initialization month, whereas in other seasons chlorophyll predictions are not possible, particularly for austral summer forecasts. The highest chlorophyll prediction skill in the austral winter and early spring correspond to the period of highest chlorophyll concentrations during which mixed layers are deepest in this predominantly nutrient-limited subtropical system (supplementary figure 3(a)). The high prediction skill in austral winter and its reappearance in the following winter are similar to a prediction pattern of extratropical sea surface temperature and chlorophyll, in which a subsurface signal remains and reemerges when the mixed layer deepens by strong seasonal wind (Alexander *et al* 1999, Stock *et al* 2015, Park *et al* 2019). Indeed, the temporal evolution of subsurface chlorophyll anomalies regressed onto surface chlorophyll shows that significant chlorophyll signals remain evident beneath the mixed layer during summer and reemerge when the mixed layer deepens

during the subsequent fall and winter (supplementary figure 4).

In the Somali coast, significant chlorophyll prediction skill is generally limited up to lead time of 1.5 years (figure 1(b)). Unlike Agulhas region, predictions of both austral summer and winter are possible within short lead time, and skill is relatively high for predictions of late austral summer and early fall (January–April). This coincides with two periods of peak chlorophyll concentration (i.e. austral summer and winter) in this region, in which primary productivity is controlled by wind-driven mixing and consequent nutrient entrainment from deeper water (supplementary figure 3(b)) (Veldhuis *et al* 1997). Note that detrending the data has little effect on the chlorophyll prediction skill in the two LMEs (supplementary figure 5).

The skill of chlorophyll predictions can also be seen in the interannual time series of satellite chlorophyll anomalies in Agulhas and Somali LMEs, where observed patterns are well predicted from January-initialized prediction at longer leads, i.e. 21 months and 20 months leads, respectively (figures 1(c) and (d)). This temporal chlorophyll variability is found not to be dominated by a certain area of the LMEs, given strong covarying relationships of chlorophyll within the LME systems (supplementary figure 6). The long-lead prediction is largely dominated by the high chlorophyll in 2002–2003 that corresponds with increased small pelagic fish catches during this period (Hutchings *et al* 2009), implying the potential utility for marine resource application as seen in a recent study (Park *et al* 2019). The skillful LME-scale prediction is particularly encouraging, given the coarse resolution of ocean grids in this global ESM that limits the simulation of coastal circulation and ecosystem processes. This indicates that LME-scale chlorophyll variability in these regions is substantially controlled by large-scale physical and biogeochemical dynamics at least for the two year prediction horizon.

3.2. Mechanisms of chlorophyll prediction skill

To understand the dynamics underlying chlorophyll prediction skill, the temporal evolutions of upper ocean (0–200 m) nitrate anomaly patterns associated with chlorophyll variations in the two LMEs are examined (figure 2). Macronutrients such as nitrate, phosphate and silicate have been found to have an important influence on phytoplankton growths in these systems (Smith and Codispoti 1980, Barlow *et al* 2020), thus we analyzed nitrate as a proxy for nutrient variability associated with chlorophyll prediction skill (supplementary figure 7). The basin-scale patterns of predicted nitrate anomalies regressed onto Agulhas satellite chlorophyll show that significant positive nitrate anomalies propagate westward from the central Indian Ocean. The positive predicted nitrate anomalies centered around 80° E, 20 months ahead of the September forecast

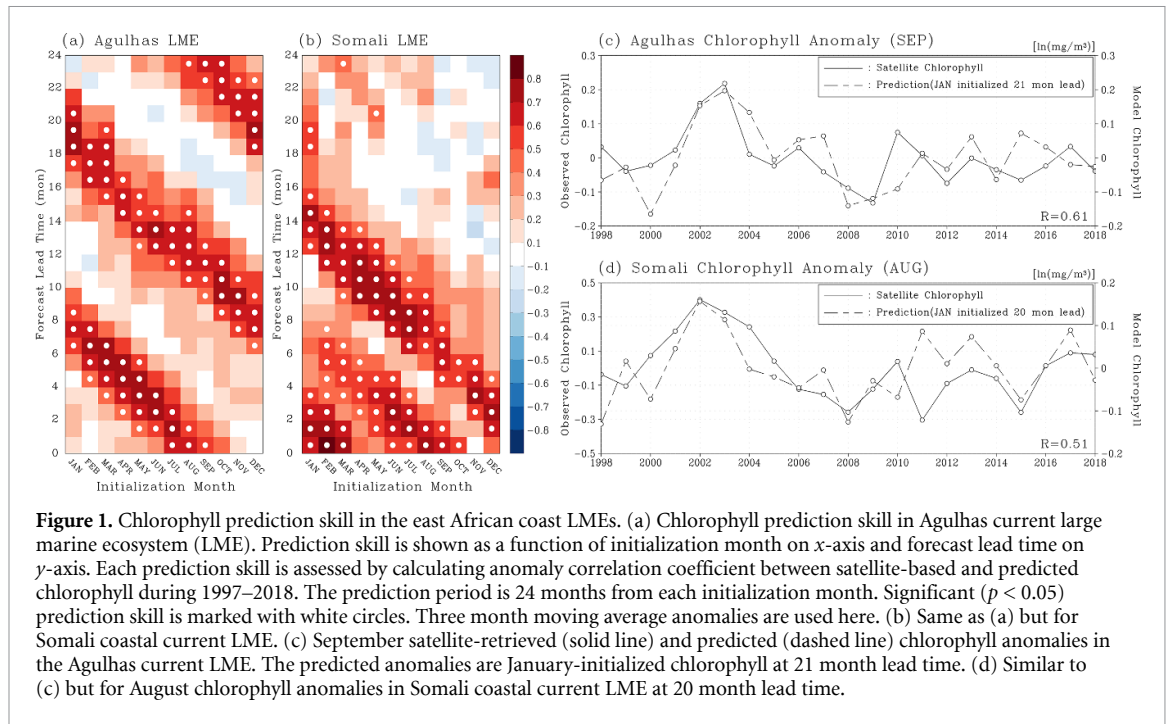


Figure 1. Chlorophyll prediction skill in the east African coast LMEs. (a) Chlorophyll prediction skill in Agulhas current large marine ecosystem (LME). Prediction skill is shown as a function of initialization month on x-axis and forecast lead time on y-axis. Each prediction skill is assessed by calculating anomaly correlation coefficient between satellite-based and predicted chlorophyll during 1997–2018. The prediction period is 24 months from each initialization month. Significant ($p < 0.05$) prediction skill is marked with white circles. Three month moving average anomalies are used here. (b) Same as (a) but for Somali coastal current LME. (c) September satellite-retrieved (solid line) and predicted (dashed line) chlorophyll anomalies in the Agulhas current LME. The predicted anomalies are January-initialized chlorophyll at 21 month lead time. (d) Similar to (c) but for August chlorophyll anomalies in Somali coastal current LME at 20 month lead time.

window, propagate westward as the forecast window is approached (figures 2(a)–(c)), and then spread both north and south along the western boundary (figures 2(d) and (e)). This eventually increases upper ocean nitrate and chlorophyll in the Agulhas system, providing a key source of chlorophyll prediction skill.

Large-scale evolution of nitrate anomalies linked to Somali chlorophyll prediction exhibit similar propagation behavior (figures 2(f)–(j)). The zonally elongated positive nitrate anomaly appears in the central Indian Ocean at 19 months lag, and the center of nitrate anomaly propagates westward and then spread to Somali system during the 19 months. The concurrent connection between nitrate and chlorophyll anomalies in the Somali LME is lower than that in the Agulhas, which is potentially a reflection of the coastally-restricted Somali system and the prominence of monsoonal wind, and river discharge forcing which may partially confound predictable signals arriving from the ocean basin (Halpern and Woiceshyn 2001, Mutia et al 2021).

The westward moving nitrate signal across the Indian Ocean represents the off-equatorial oceanic Rossby wave slowly propagating from the eastern Indian Ocean to the west. This wave signal found in the biogeochemical variable is consistent with coupled Rossby waves observed in physical variables, such as sea level or upper ocean heat contents in the Indian Ocean (White 2000, Jury and Huang 2004). The slow phase speed of Rossby waves in this off-equatorial region is due to the inverse relationship between phase speed and latitude, thus it takes 2–3 years to cross the Indian Ocean at 15° S (Perigaud and Delecluse 1993). Consistent with this,

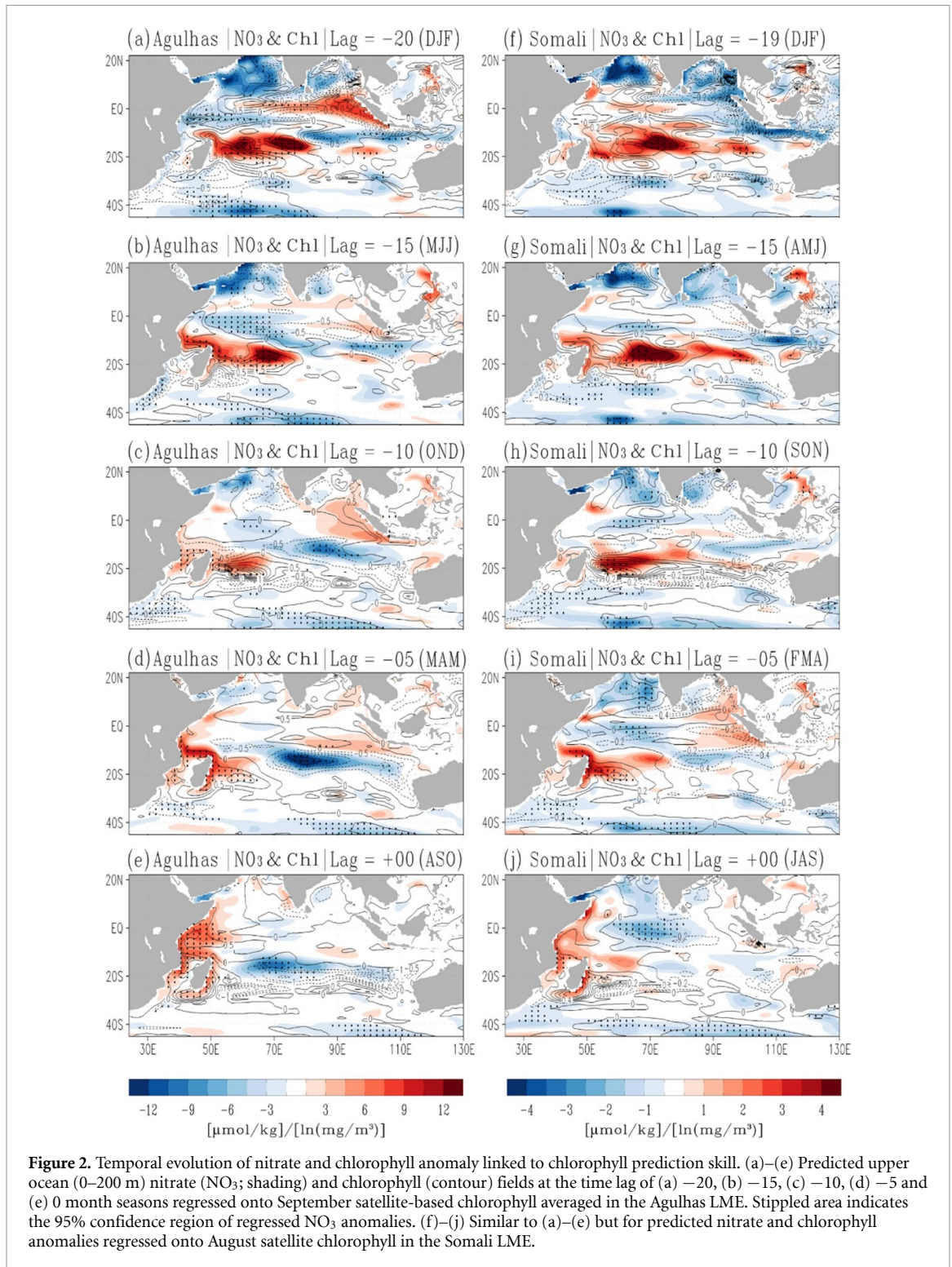
the propagation speed of nitrate anomalies found in figure 2 is approximately 0.08 m s^{-1} .

The Rossby wave signal shown in the nitrate anomalies in the Indian Ocean implies that this physical oceanic phenomenon provides a basis for predicting ocean biogeochemical variables in the two African coast LMEs. The upwelling Rossby wave supplies nutrient to the euphotic layer, and its slowly moving signal together with reemergence of subsurface nutrient anomalies during periods of peak mixing and chlorophyll in these tropical and subtropical LMEs allows the prediction of coastal chlorophyll at longer leads. Skill diminishes when surface chlorophyll is suppressed by strong stratification over the austral summer and adjacent months.

3.3. Rossby wave initiated by El Niño/Southern Oscillation (ENSO)-Indian Ocean teleconnection

What mechanisms are associated with the initiation of upwelling Rossby wave and associated nitrate anomalies in the Indian Ocean? To identify the physical process, the analysis for the temporal evolution of large-scale dynamics is extended up to four years before the increase in Agulhas chlorophyll anomalies. For this, we used the reconstructed physical and biogeochemical fields from the ensemble-coupled data assimilation system integrating with the global marine biogeochemical model (i.e. ECDA-COBALT), which has been used for the initialization of our two year-long prediction run (Park et al 2019).

The zonal propagation of nitrate anomalies in the central Indian Ocean are well depicted in Hovmöller diagram of nitrate anomalies averaged over the latitudinal band 20° – 10° S (figure 3(a)). The significant positive nitrate anomalies found in figure 2(a)



started about 42 months before the increase in Agulhas chlorophyll. The westward moving nitrate anomalies take about 2–3 years to reach the western boundary and they experience disruptions and enhancements during the propagation period, presumably due to the interplay between the Rossby wave signal and other sources of nitrate variability.

The regressed fields of physical and biogeochemical variables onto the satellite chlorophyll in the Agulhas system show that the initial positive nitrate

signals are triggered and amplified by two consecutive La Niña-like patterns at around lag 42 and 32 months (figures 3(b) and (c)), which is consistent with the result shown in figure 3(a). At the time lag of 42 months, a weak La Niña signal in the equatorial Pacific is captured with cyclonic wind stress anomalies over the southeastern Indian Ocean. This low-level wind perturbation is consistent with a Gill-type response to diabatic warming caused by the eastern Indian Ocean precipitation anomalies (Gill 1980). This is further

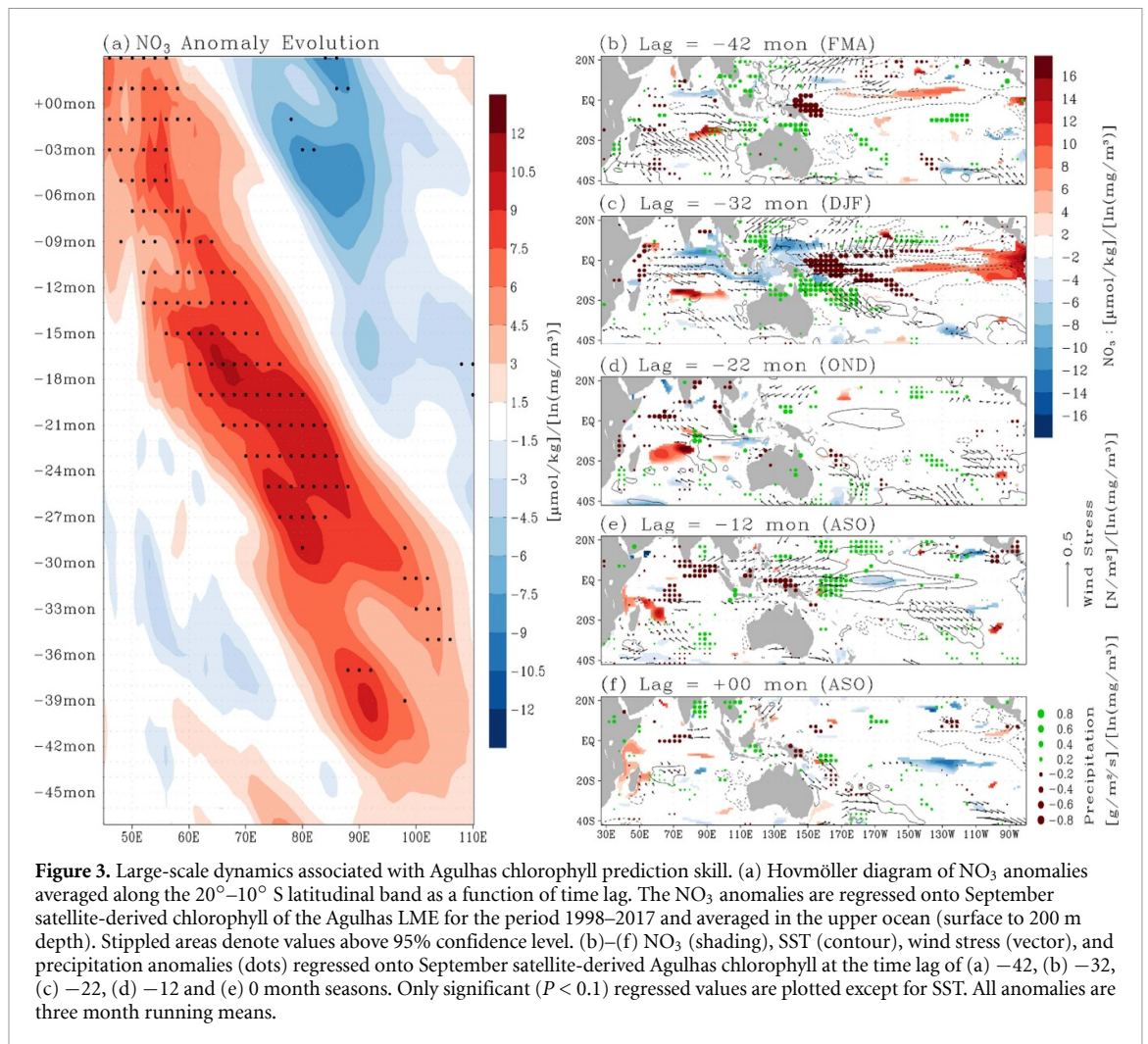
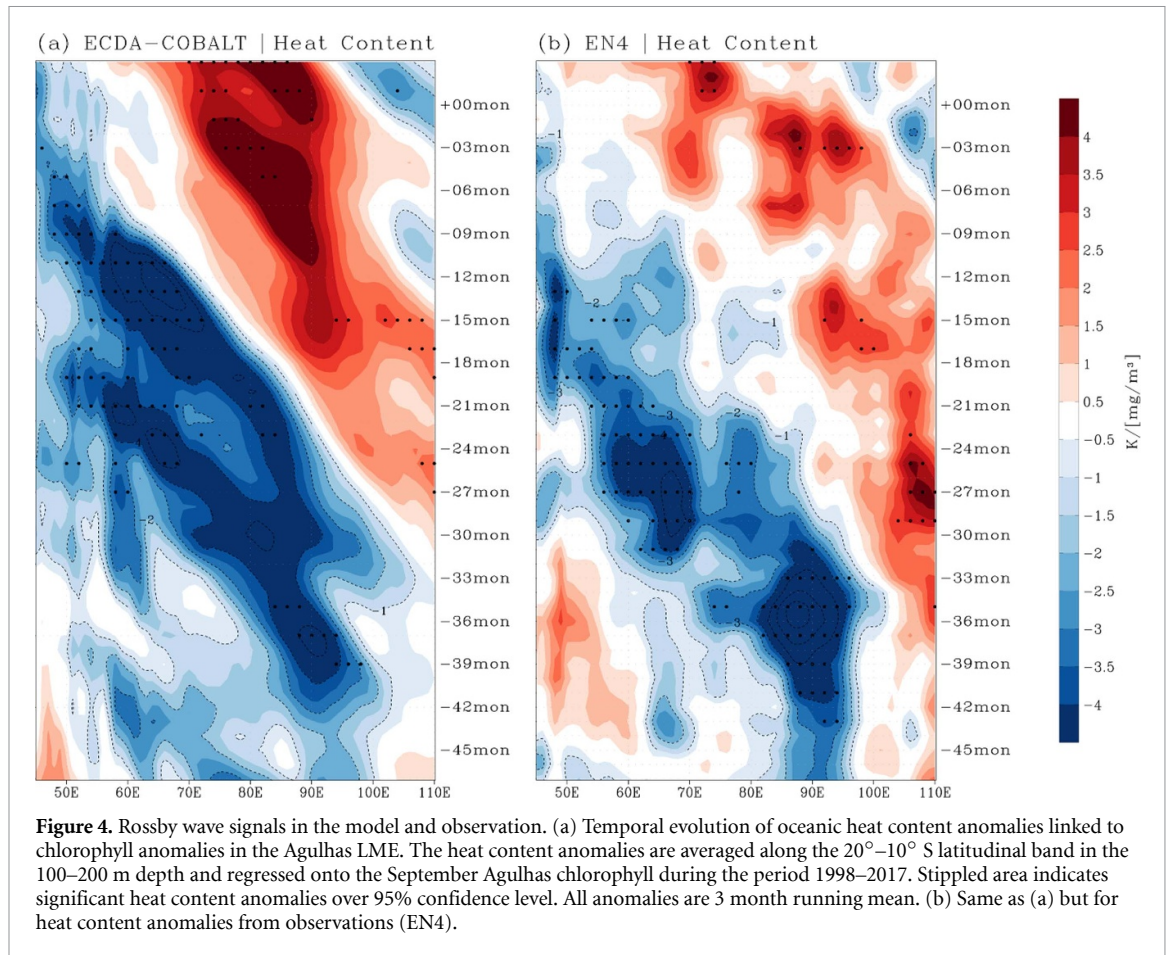


Figure 3. Large-scale dynamics associated with Agulhas chlorophyll prediction skill. (a) Hovmöller diagram of NO₃ anomalies averaged along the 20°–10° S latitudinal band as a function of time lag. The NO₃ anomalies are regressed onto September satellite-derived chlorophyll of the Agulhas LME for the period 1998–2017 and averaged in the upper ocean (surface to 200 m depth). Stippled areas denote values above 95% confidence level. (b)–(f) NO₃ (shading), SST (contour), wind stress (vector), and precipitation anomalies (dots) regressed onto September satellite-derived Agulhas chlorophyll at the time lag of (a) –42, (b) –32, (c) –22, (d) –12 and (e) 0 month seasons. Only significant ($P < 0.1$) regressed values are plotted except for SST. All anomalies are three month running means.

supported by an idealized model experiment using a linear baroclinic model (Watanabe and Kimoto 2000) forced by a prescribed diabatic heating over the eastern Indian Ocean at around 110° E, 15° S (supplementary figure 8). The cyclonic winds can, in turn, lead to the increase in upper ocean nitrate through the upwelling of nutrient-rich waters. A similar feature is also found at the time lag of 32 months (figure 3(b)). That is, a strong La Nina signal increases the precipitation in the eastern Indian Ocean, and then it generates cyclonic flow in the southern subtropical Indian Ocean, leading to the increase in upwelling and nitrate. The nitrate anomalies propagate westward with time and finally reach the western boundary at 0 month lag (figure 3(f)). Such westward nitrate propagation pattern is commonly detected after major La Niña events despite minor discrepancies in its magnitude and structure, and also detected after El Niño events with a reversed sign of nitrate anomalies (supplementary figures 9 and 10). Overall inter-basin interacting processes associated with Agulhas chlorophyll prediction skill are also found in the observation-based datasets (supplementary figure 11).

Previous work has shown that Indian Ocean dipole (IOD) events are accompanied by a westward-propagating Rossby wave in the southern tropical Indian Ocean generated by wind stress forcing factors (Masumoto and Meyers 1998, Vinayachandran *et al* 2002), implying the potential role of IOD in chlorophyll prediction skill. The ESM-based prediction system used here shows significant IOD prediction skill within 1.5 year prediction horizon, however, chlorophyll variability in the Agulhas system generally shows a less significant correlation with IOD index compared to ENSO index (supplementary figure 12). The strong correlation between ENSO and Agulhas chlorophyll at long time lags indicates a primary role of ENSO-Indian Ocean teleconnection in initiating slowly moving subtropical Rossby wave and subsequent chlorophyll variability in the western boundary. In the Somali system, however, chlorophyll is significantly correlated with IOD particularly for short time lags, with a significant correspondence with ENSO for longer time lags. This implies that Somali chlorophyll is affected by both ENSO and IOD and/or their co-variability.



Lastly, we examine whether the westward moving Rossby wave signal linked to Agulhas chlorophyll anomalies is identified in the observation. The observed ocean temperature analyzed here is from the EN4 objective analyses data (Good *et al* 2013). The ocean temperature averaged in the 100–200 m depth, i.e. oceanic heat content, is used to diagnose the upwelling Rossby wave that transports nitrate signal to the western Indian Ocean. In both model and observation, the heat content anomalies regressed onto satellite chlorophyll in the Agulhas region shows the significant negative anomalies initiated four years before the increase in Agulhas chlorophyll, and this negative signal moves westward afterward (figure 4). The westward-moving heat content anomalies linked to Agulhas chlorophyll are also present in the predicted ocean temperature (supplementary figure 13). The overall results here imply that despite some discrepancies between model and observations, the ESM used here captures the basin-wide physical processes and its accompanying biogeochemical responses, which is a key source of chlorophyll prediction skill in the western Indian Ocean LMEs.

4. Discussion and conclusion

The ESM-based marine biogeochemical prediction system used in the present study shows significant

skill in predicting satellite-derived chlorophyll fluctuations in the east African coastal regions. The skillful chlorophyll prediction arises primarily from successfully simulating coupling processes between atmosphere, ocean, and marine biogeochemistry in the Indian Ocean. The inter-basin interacting process between atmosphere and ocean exemplifies the compelling predictive potential of global ESM even for regional biogeochemical prediction, while regional model-based prediction systems may be limited in predicting such inter-basin process. This result is similar to enhanced prediction of climate variability by incorporating inter-basin precursors (Ham *et al* 2013, Cai *et al* 2019).

The ESM-based biogeochemical prediction system can extend beyond chlorophyll such as oxygen, net primary production, and zooplankton. Successful prediction of these key biogeochemical variables may provide richer information on the linkage between bottom-up drivers and fisheries production and its mechanistic principles across globally distributed ecosystems, thus offering considerable potential for anticipatory dynamic management of marine resources (Tommasi *et al* 2017). Realizing the full potential of global earth system predictions for marine ecosystem and resource applications, however, will require a range of modeling and observational advances. The lack of global-scale biogeochemical

observations often hinders the generation of optimal biogeochemical initialization data and the validation assessment of model products. In this regard, assimilating the remotely sensed ocean color and the recently available biogeochemical Argo floats data into the ESM can bring additional gains in biogeochemical prediction skill and may eventually provide a robust time series for reforecast verification. Recent studies support this point by showing the improvement of biogeochemical reanalysis from biogeochemical assimilation and the degradation of biogeochemical predictions from the perturbations in biogeochemical initial conditions (Ciavatta *et al* 2014, Ford and Barciela 2017, Salon *et al* 2019, Ford 2021).

Future inclusion of dynamic river nutrient fluxes into the ESM may also improve the coastal biogeochemical prediction skill given that coastal biogeochemical cycles are substantially controlled by river nutrients (Walker and Rabalais 2006, Sigleo and Frick 2007). For example, a recent observational study showed that chlorophyll concentration in the east African coast is largely controlled by river discharge during the rainy season (Mutia *et al* 2021). In addition to the dynamic coupling between river and coastal water biogeochemistry, much higher resolution than available in the present model (1° , ~ 100 km) would be preferable to adequately represent the complex coastal physics and biogeochemistry towards improvement of the coastal chlorophyll prediction. Such high resolution models are expected to better simulate coastal retention and residence time of oceanic tracers probably due to better representation of coastal bathymetry and complex fine-scale dynamics (Liu *et al* 2019) and should be a priority for future work.

Data availability statement

The data that support the findings of this study are available upon reasonable request from the authors.

Acknowledgments

The authors would like to thank the anonymous reviewers for helpful and constructive comments on the manuscript. This work was supported by the KMA R&D Program (KMI2020-01117) and the National Research Foundation of Korea (NRF-2020R1A4A3079510).

ORCID iD

Jong-Yeon Park  <https://orcid.org/0000-0001-8125-4552>

References

- Alexander M A, Deser C and Timlin M S 1999 The reemergence of SST anomalies in the North Pacific Ocean *J. Clim.* **12** 2419–33
- Barlow R, Lamont T, Gibberd M J, Russo C, Airs R, Tutt G, Britz K and van den Berg M 2020 Phytoplankton adaptation and absorption properties in an Agulhas current ecosystem *Deep-Sea Res. I* **157** 103209
- Bonan G B and Doney S C 2018 Climate, ecosystems, and planetary futures: the challenge to predict life in Earth system models *Science* **359** 6375
- Bretherton C S, Widmann M, Dymnikov V P, Wallace J M and Blade I 1999 The effective number of spatial degrees of freedom of a time-varying field *J. Clim.* **12** 1990–2009
- Cai W J *et al* 2019 Pantropical climate interactions *Science* **363** 944
- Campbell J W 1995 The lognormal distribution as a model for bio-optical variability in the sea *J. Geophys. Res.* **100** 13237–54
- Chang Y S, Zhang S Q, Rosati A, Delworth T L and Stern W F 2013 An assessment of oceanic variability for 1960–2010 from the GFDL ensemble coupled data assimilation *Clim. Dyn.* **40** 775–803
- Cheung W W L, Sarmiento J L, Dunne J, Frolicher T L, Lam V W Y, Palomares M L D, Watson R and Pauly D 2013 Shrinking of fishes exacerbates impacts of global ocean changes on marine ecosystems *Nat. Clim. Change* **3** 254–8
- Ciavatta S, Torres R, Martinez-Vicente V, Smyth T, Dall’Olmo G, Polimene L and Allen J I 2014 Assimilation of remotely-sensed optical properties to improve marine biogeochemistry modelling *Prog. Oceanogr.* **127** 74–95
- Costello C *et al* 2016 Global fishery prospects under contrasting management regimes *Pro. Natl Acad. Sci. USA* **113** 5125–9
- Doney S C *et al* 2012 Climate change impacts on marine ecosystems *Annual Review of Marine Science* vol 4, eds C A Carlson and S J Giovannoni (San Mateo, CA: Annual Reviews) pp 11–37
- Dufresne J-L, Foujols M-A, Denvil S, Caubel A, Marti O, Aumont O, Balkanski Y, Bekki S, Bellenger H and Benshila R 2013 Climate change projections using the IPSL-CM5 Earth System Model: from CMIP3 to CMIP5 *Clim. Dyn.* **40** 2123–65
- Dunne J P, John J G, Shevliakova E, Stouffer R J, Krasting J P, Malyshev S L, Milly P, Sentman L T, Adcroft A J and Cooke W 2013 GFDL’s ESM2 global coupled climate–carbon earth system models. Part II: carbon system formulation and baseline simulation characteristics *J. Clim.* **26** 2247–67
- Dussin R, Curchitser E, Stock C and Van Oostende N 2019 Biogeochemical drivers of changing hypoxia in the California current ecosystem *Deep-Sea Res. II* **169** 104590
- Esaias W E *et al* 1998 An overview of MODIS capabilities for ocean science observations *IEEE Trans. Geosci. Remote Sens.* **36** 1250–65
- Finney B P, Alheit J, Emeis K C, Field D B, Gutierrez D and Struck U 2010 Paleocological studies on variability in marine fish populations: a long-term perspective on the impacts of climatic change on marine ecosystems *J. Mar. Syst.* **79** 316–26
- Ford D A and Barciela R M 2017 Global marine biogeochemical reanalyses assimilating two different sets of merged ocean colour products *Remote Sens. Environ.* **203** 40–54
- Ford D 2021 Assimilating synthetic Biogeochemical-Argo and ocean colour observations into a global ocean model to inform observing system design *Biogeosciences* **18** 509–34
- Frolicher T L, Ramseier L, Raible C C, Rodgers K B and Dunne J 2020 Potential predictability of marine ecosystem drivers *Biogeosciences* **17** 2061–83
- Gill A E 1980 Some simple solutions for heat-induced tropical circulation *Q. J. R. Meteorol. Soc.* **106** 447–62
- Glibert P M, Icarus Allen J, Artioli Y, Beusen A, Bouwman L, Harle J, Holmes R and Holt J 2014 Vulnerability of coastal ecosystems to changes in harmful algal bloom distribution in response to climate change: projections based on model analysis *Glob. Change Biol.* **20** 3845–58
- Good S A, Martin M J and Rayner N A 2013 EN4: quality controlled ocean temperature and salinity profiles and

- monthly objective analyses with uncertainty estimates *J. Geophys. Res.* **118** 6704–16
- Halpern D and Woiceshyn P M 2001 Somali jet in the Arabian Sea, El Niño, and India rainfall *J. Clim.* **14** 434–41
- Ham Y-G, Kug J-S, Park J-Y and Jin F-F 2013 Sea surface temperature in the north tropical Atlantic as a trigger for El Niño/Southern Oscillation events *Nat. Geosci.* **6** 112–6
- Hutchings L, Van der Lingen C, Shannon L, Crawford R, Verheye H, Bartholomae C, Van der Plas A, Louw D, Kreiner A and Ostrowski M 2009 The Benguela current: an ecosystem of four components *Prog. Oceanogr.* **83** 15–32
- Jury M R and Huang B 2004 The Rossby wave as a key mechanism of Indian Ocean climate variability *Deep-Sea Res. I* **51** 2123–36
- Kanamitsu M, Ebisuzaki W, Woollen J, Yang S K, Hnilo J J, Fiorino M and Potter G L 2002 NCEP-DOE AMIP-II reanalysis (R-2) *Bull. Am. Meteorol. Soc.* **83** 1631–43
- Kwiatkowski L, Torres O, Bopp L, Aumont O, Chamberlain M, Christian J R, Dunne J P, Gehlen M, Ilyina T and John J G 2020 Twenty-first century ocean warming, acidification, deoxygenation, and upper-ocean nutrient and primary production decline from CMIP6 model projections *Biogeosciences* **17** 3439–70
- Lindsay K, Bonan G B, Doney S C, Hoffman F M, Lawrence D M, Long M C, Mahowald N M, Keith Moore J, Randerson J T and Thornton P E 2014 Preindustrial-control and twentieth-century carbon cycle experiments with the Earth system model CESM1 (BGC) *J. Clim.* **27** 8981–9005
- Liu X, Dunne J P, Stock C A, Harrison M J, Adcroft A and Resplandy L 2019 Simulating water residence time in the coastal ocean: a global perspective *Geophys. Res. Lett.* **46** 13910–9
- Masumoto Y and Meyers G 1998 Forced Rossby waves in the southern tropical Indian Ocean *J. Geophys. Res.* **103** 27589–602
- McClain C R, Cleave M L, Feldman G C, Gregg W W, Hooker S B and Kuring N 1998 Science quality SeaWiFS data for global biosphere research *Sea Technol.* **39** 10–16
- Ménard F, Lorrain A, Potier M and Marsac F 2007 Isotopic evidence of distinct feeding ecologies and movement patterns in two migratory predators (yellowfin tuna and swordfish) of the western Indian Ocean *Mar. Biol.* **153** 141–52
- Mutia D, Carpenter S, Jacobs Z, Jebri F, Kamau J, Kelly S J, Kimeli A, Langat P K, Makori A and Nencioli F 2021 Productivity driven by Tana river discharge is spatially limited in Kenyan coastal waters *Ocean Coast. Manage.* **211** 105713
- Park J Y, Stock C A, Yang X, Dunne J P, Rosati A, John J and Zhang S 2018 Modeling global ocean biogeochemistry with physical data assimilation: a pragmatic solution to the equatorial instability *J. Adv. Model. Earth Syst.* **10** 891–906
- Park J-Y, Stock C A, Dunne J P, Yang X and Rosati A 2019 Seasonal to multiannual marine ecosystem prediction with a global Earth system model *Science* **365** 284–8
- Perigaud C and Delecluse P 1993 Interannual sea level variations in the tropical Indian Ocean from Geosat and shallow water simulations *J. Phys. Oceanogr.* **23** 1916–34
- Reynolds R W, Smith T M, Liu C, Chelton D B, Casey K S and Schlax M G 2007 Daily high-resolution-blended analyses for sea surface temperature *J. Clim.* **20** 5473–96
- Salon S, Cossarini G, Bolzon G, Feudale L, Lazzari P, Teruzzi A, Solidoro C and Crise A 2019 Novel metrics based on Biogeochemical Argo data to improve the model uncertainty evaluation of the CMEMS mediterranean marine ecosystem forecasts *Ocean Sci.* **15** 997–1022
- Seferian R, Bopp L, Gehlen M, Swingedouw D, Mignot J, Guilyardi E and Servonnat J 2014 Multiyear predictability of tropical marine productivity *Pro. Natl Acad. Sci. USA* **111** 11646–51
- Sherman K 1991 The large marine ecosystem concept: research and management strategy for living marine resources *Ecol. Appl.* **1** 349–60
- Sherman K 2014 Adaptive management institutions at the regional level: the case of large marine ecosystems *Ocean Coast. Manage.* **90** 38–49
- Sigleo A and Frick W 2007 Seasonal variations in river discharge and nutrient export to a Northeastern Pacific estuary *Estuar. Coast. Shelf Sci.* **73** 368–78
- Smith S L and Codispoti L A 1980 Southwest monsoon of 1979: chemical and biological response of somali coastal waters *Science* **209** 597–600
- Stock C A, Dunne J P and John J G 2014a Drivers of trophic amplification of ocean productivity trends in a changing climate *Biogeosciences* **11** 7125–35
- Stock C A, Dunne J P and John J G 2014b Global-scale carbon and energy flows through the marine planktonic food web: an analysis with a coupled physical-biological model *Prog. Oceanogr.* **120** 1–28
- Stock C A, Pegion K, Vecchi G A, Alexander M A, Tommasi D, Bond N A, Fratantoni P S, Gudgel R G, Kristiansen T and O'Brien T D 2015 Seasonal sea surface temperature anomaly prediction for coastal ecosystems *Prog. Oceanogr.* **137** 219–36
- Taboada F G, Barton A D, Stock C A, Dunne J and John J G 2019 Seasonal to interannual predictability of oceanic net primary production inferred from satellite observations *Prog. Oceanogr.* **170** 28–39
- Tommasi D, Stock C A, Pegion K, Vecchi G A, Methot R D, Alexander M A and Checkley D M 2017 Improved management of small pelagic fisheries through seasonal climate prediction *Ecol. Appl.* **27** 378–88
- Veldhuis M J, Kraay G W, Van Bleijswijk J D and Baars M A 1997 Seasonal and spatial variability in phytoplankton biomass, productivity and growth in the northwestern Indian Ocean: the southwest and northeast monsoon, 1992–1993 *Deep-Sea Res. I* **44** 425–49
- Vinayachandran P N, Iizuka S and Yamagata T 2002 Indian Ocean dipole mode events in an ocean general circulation model *Deep-Sea Res. II* **49** 1573–96
- Vousden D 2016 Productivity and biomass assessments for supporting management of the Agulhas current and Somali current large marine ecosystems *Environ. Dev.* **17** 118–25
- Walker N D and Rabalais N N 2006 Relationships among satellite chlorophyll a, river inputs, and hypoxia on the Louisiana continental shelf, Gulf of Mexico *Estuar. Coasts* **29** 1081–93
- Watanabe M and Kimoto M 2000 Atmosphere-ocean thermal coupling in the North Atlantic: a positive feedback *Q. J. R. Meteorol. Soc.* **126** 3343–69
- Watanabe S, Hajima T, Sudo K, Nagashima T, Takemura T, Okajima H, Nozawa T, Kawase H, Abe M and Yokohata T 2011 MIROC-ESM 2010: model description and basic results of CMIP5-20c3m experiments *Geosci. Model Dev.* **4** 845–72
- White W B 2000 Coupled Rossby waves in the Indian Ocean on interannual timescales *J. Phys. Oceanogr.* **30** 2972–88